Modelling of late Quaternary climate over Asia: a synthesis

ANDREW B. G. BUSH

BOREAS

Bush, A. B. G. 2004 (May): Modelling of late Quaternary climate over Asia: a synthesis. *Boreas*, Vol. 33, pp. 155–163. Oslo. ISSN 0300-9483.

Through the late Quaternary, the global climate system ranged from full glacial to temperate interglacial conditions. On a smaller spatial scale, regional climates of the late Quaternary exhibited fluctuations that were at times asynchronous to these global changes. For example, glacier expansion in the Himalayas during the mid-Holocene appears to be at odds with the notion of increased global temperature. A clear understanding of the dynamical processes governing regional climate is therefore essential to the correct interpretation of proxy climate data. We summarize results from numerical simulations of the Last Glacial Maximum (LGM) and the mid-Holocene, and focus on the multiple processes that control regional climate of the Himalaya and surrounding areas, with emphasis on monsoon dynamics and variability. It is shown that changes in the south Asian monsoon (caused by fluctuations in Earth's orbital parameters, by tropical Pacific Ocean temperatures, or by exposure of the Sunda shelf) alter the hydrological balance in regions bordering the Tibetan Plateau, a balance for which there are extensive continental proxy records. Numerical results correlate with the expansion/contraction cycles of deserts near the Chinese Loess Plateau. In addition, the LGM monsoon exhibits significant snow accumulation in the eastern Himalaya, whereas the mid-Holocene monsoon exhibits increased accumulation in the northwestern Himalaya. Simulated changes are therefore in accord with field data and demonstrate that numerical simulations can be a useful tool in the interpretation of regional proxy data, particularly when those data are asynchronous to global records.

Andrew B. G. Bush (e-mail: andrew.bush@ualberta.ca), Department of Earth and Atmospheric Sciences, University of Alberta, Edmonton, Alberta, Canada T6G 2E3; *received 1st July 2003, accepted 10th December 2003.*

The late Quaternary is a time period upon which many modelling studies have focused because of the wealth of proxy data available from a variety of sources such as corals (Guilderson *et al.* 1994), pore fluids (Schrag *et al.* 1996), ground water (Stute *et al.* 1995), ice cores (Thompson *et al.* 1995), pollen (e.g. Colinvaux *et al.* 1996), paleolimnology (e.g. Kuzmin *et al.* 1997), loess/paleosol sequences (e.g. Rutter 1992; Ding *et al.* 1999), lake sediments (e.g. Lamoureux *et al.* 2001; Colman *et al.* 1995), and terrestrial vegetation (e.g. Prentice & Webb 1998; MacDonald *et al.* 2000). These data can be used to estimate past climatic conditions, but they can also be used to verify results from numerical simulations of paleoclimate. Such model-data intercomparisons are necessary in order to determine the verisimilitude of numerical calculations (e.g. Broccoli & Marciniak 1996; Prentice *et al.* 1998; Pinot *et al.* 1999; Mahowald *et al.* 1999; Braconnot *et al.* 2000; Bush *et al.* 2002; Kageyama *et al.* 2001). The advantage of general circulation model (GCM) simulations, however, is that model results may be diagnosed in order to understand the atmospheric dynamics underlying regional climate change, and they can also be used to determine the sensitivity of climate to proposed changes in surface boundary conditions such as sea surface temperature (SST; Keshavamurty 1982; Rind & Peteet 1985; Bush 2001a).

The Last Glacial Maximum (LGM), in particular, has received an enormous amount of attention from the modelling community because of the radical difference between its climate and that of today. Initial modelling attempts were able to determine the climatic impact of LGM continental ice, atmospheric CO_2 and surface albedo (e.g. Manabe & Hahn 1977; Manabe & Broccoli 1985; Broccoli & Manabe 1987). Subsequent studies demonstrated that the dynamics of a glacial atmosphere are significantly different from those of today, particularly in the northern hemisphere storm tracks (e.g. Hall *et al.* 1996). Recently, a variety of coupled atmosphere–ocean GCMs have been applied to the LGM in order to determine the ocean's role in maintaining, and perhaps evolving, the glacial climate (Weaver *et al.* 1998; Bush & Philander 1999; Kitoh *et al.* 2001).

Similarly, the mid-Holocene has been a focus for the modelling community because it represents a time during which the surface boundary conditions were comparable to today's, but the incoming solar radiation was quite different given the Earth's orbital configuration at the time (Berger 1992; Berger & Loutre 1991). Simulations of the mid-Holocene therefore represent relatively clean experiments from which the direct relationship between solar forcing, climate and atmosphere–ocean dynamics may be quantified (e.g. Kutzbach & Otto-Bleisner 1982; Kutzbach & Guetter 1986; Prell & Kutzbach 1992; Otto-Bleisner 1999; Bush 1999).

The LGM and the mid-Holocene are therefore a focus for the numerical experiments to be presented here. The sections to follow describe simulation results as they pertain to the climate and hydrology over Asia at the LGM and during the mid-Holocene, and what implications these results may have for glaciation and drainage.

Taylor & Francis
Taylor & Francis Group

DOI 10.1080/03009480410001073

While our primary focus is on Asian climate, results from the tropics are also described because of the atmospheric teleconnections that link the tropical Pacific with the Asian monsoon. Some details of the numerical models used for the simulations are given first, followed by a summary and discussion of the results.

Numerical models

Full details of the atmospheric GCM may be found in Gordon & Stern (1982). Particular configurations that were used in the Holocene and LGM simulations are outlined here. The global model is spectral in the horizontal with rhomboidal truncation at wavenumber 30, which translates into an equivalent spatial resolution of 3.75° in longitude by 2.25° in latitude at the equator. There are 14 unevenly spaced levels in the vertical, with higher vertical resolution in the planetary boundary layer (lower kilometer) and near the tropopause. Clouds are predicted according to the scheme outlined in Wetherald & Manabe (1988). Land surface albedo values are specified to reflect existing vegetation (or lack thereof) but may be changed during the course of an integration by the presence of snow.

In the atmosphere-only simulations, monthly mean SST is specified and interpolated to daily values during the course of the integration. For modern SST, values are specified using data from Levitus (1982). In the coupled atmosphere–ocean simulations, the ocean model is the one developed at the Geophysical Fluid Dynamics Laboratory in Princeton, NJ (Pacanowski *et al.* 1991) with a spatial resolution of 3.62° in longitude by 2° in latitude. There are 15 levels in the vertical with higher vertical resolution in the upper ocean. Sea ice is predicted according to the thermodynamic formulation of Fanning & Weaver (1996) and includes brine rejection. The albedo of sea ice is specified depending on ice thickness and surface temperature, with higher values for thicker ice under a colder atmosphere.

In the coupled model simulations, the atmospheric and oceanic models interact dynamically and thermodynamically and pass required boundary condition information at 1-day intervals. Boundary conditions required by the atmosphere model are daily mean SST, surface current velocities and sea ice extent. Boundary conditions required by the ocean model are daily mean vector wind stress, net heat flux, net freshwater flux, net shortwave radiation and sea ice extent. The ocean is initially at rest with temperature and salinity fields specified from modern observational data (Levitus 1982). Given the time required to integrate the coupled model, results to be presented are from decadal timescale simulations and focus only on the surface–ocean and the atmosphere–ocean dynamics that change SST and surface currents. It would be desirable to continue the simulations further in order to study changes in the deep ocean circulation, but this is at present beyond the scope of these studies.

In the mid-Holocene simulations, atmospheric CO_2 is fixed at 300 ppm and modern values of topography, sea level and land surface albedo are imposed. In the early Holocene simulations, remnants of the Laurentide Ice Sheet are taken into account by specifying a higher albedo over the area covered by ice, and by modifying surface topography according to the reconstructions by Peltier (1994).

In the LGM simulation, atmospheric CO_2 is fixed at 200 ppm. LGM ice sheet albedo and topography are imposed where necessary (Peltier 1994), and continental boundaries are set assuming a 120 m drop in sea level (Fairbanks 1989). LGM land surface albedo is specified according to CLIMAP (1981) reconstructions.

In all simulations, seasonal solar insolation is computed using appropriate values for obliquity, eccentricity and longitude of perihelion (Berger 1992; Berger & Loutre 1991). Simulations were performed for today's configuration and the results from these control runs are referred to as the present-day climate. Unless otherwise noted, results shown are from the coupled model simulations.

Simulated Asian climate in the late Quaternary

In the mid-Holocene simulation, annual mean surface temperatures across northern Asia are warmer than present and exhibit a stronger seasonal cycle (Fig. 1A, C; the amplitude of the seasonal cycle is defined here as the difference between the average June-July-August temperature and the average December-January-February temperature). A stronger seasonal cycle in the Asian continental interior is consistent with the more seasonal radiative forcing associated with high obliquity and a summertime perihelion (e.g. Kutzbach & Guetter 1986; Kutzbach & Otto-Bleisner 1982). Across southern Asia and tropical Africa, however, temperatures are cooler and are related to the tropical cooling associated with a more La Niña-like mean state in the tropical Pacific Ocean (Bush 1999).

In the LGM simulation, annual mean temperatures are colder everywhere (typically 6–8°C colder than today in the Asian interior) but particularly so in the vicinity of the Fennoscandian ice sheet (Fig. 1B). A very large increase in the amplitude of the seasonal cycle (Fig. 1D) is caused primarily by exceptionally cold wintertime temperatures over Siberia. Tropical temperatures that are $\sim$4° colder than today are also simulated, with $\sim$7° of cooling over tropical mountains. Some of this cooling is associated with reduced atmospheric CO_2 and some with reduced water vapour content (global mean specific humidity is less than today by approximately 10%). In addition, however,

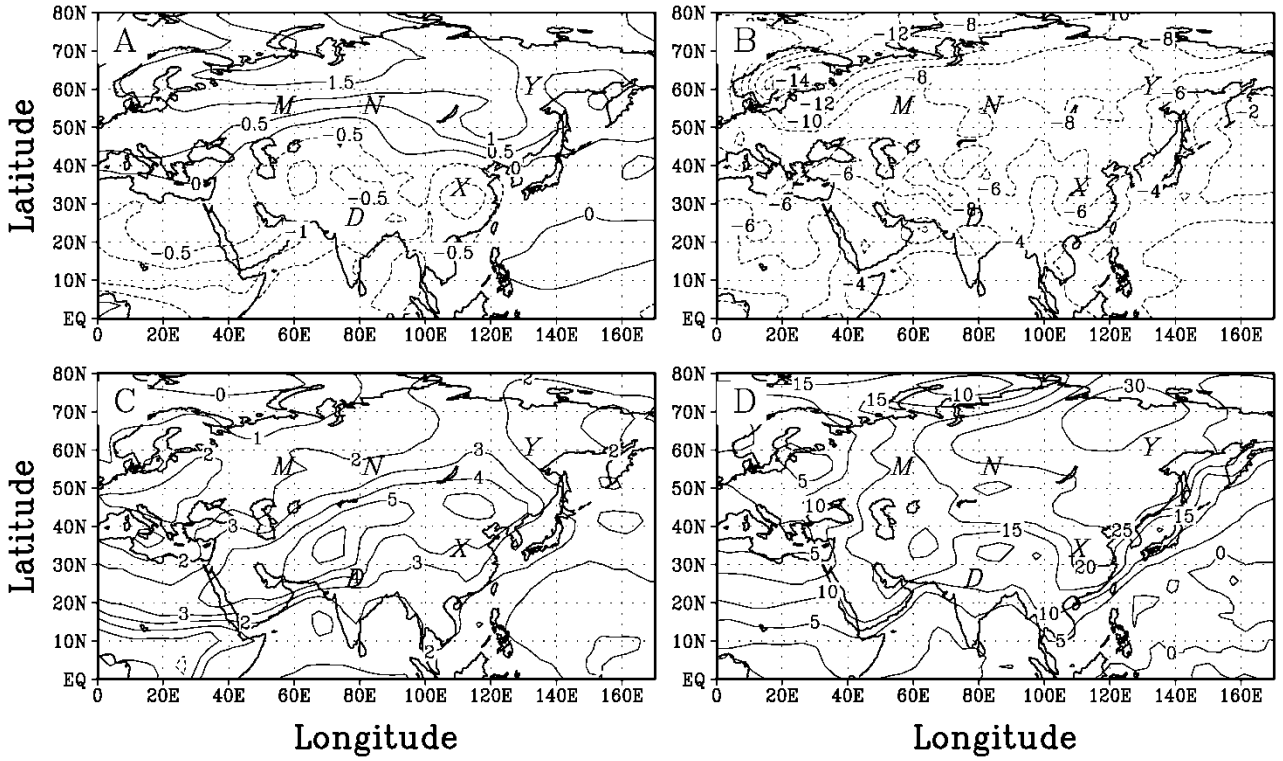

Fig. 1. Annual mean temperature difference (experiment minus control) for (A) the mid-Holocene and (B) the LGM. The contour interval in (A) is 0.5° and in (B) it is 2°C. (C) and (D) show the difference (experiment minus control) in amplitude of the seasonal cycle (i.e. the difference in temperature between mean summer conditions (June-July-August) and mean winter conditions (December-January-February)) for the mid-Holocene and the LGM, respectively. The contour interval in (C) is 1° and in (D) it is 5°C. Note: In all panels and in all subsequent figures the following geographic locations are marked for reference: Moscow (M), Novosibirsk (N), Yakutsk (Y), Xian (X), and Delhi (D).

stronger trade winds over the Pacific Ocean increase oceanic upwelling and decrease SST such that temperatures over the western Pacific are up to 6° colder than present (Bush & Philander 1998). These cold temperatures, though regional in extent, are supported by evidence for extensive snow line depressions over east Africa and New Guinea (Rind & Peteet 1985; Hope *et al.* 1976) as well as by the continental data that indicate 5–6° of cooling (Guilderson *et al.* 1994; Stute *et al.* 1995; Thompson *et al.* 1995). Indeed, cooling over the tropical continents cannot reach the degree inferred from some of the proxy data without some regions of the tropical oceans having SST colder than the CLIMAP (1981) reconstructions (Rind & Peteet 1985).

Of central importance to Asia's drainage network in the Late Quaternary are changes in the hydrological cycle. Changes in precipitation, evaporation, snow accumulation and soil moisture play crucial roles in, for example, glacier build-up and the movements of deserts. Each of these simulated variables will be examined in turn.

Annual mean precipitation in the mid-Holocene simulation is much greater over the Himalaya because of stronger summer monsoon winds that enhance evaporation over the Arabian Sea and bring more moisture further inland (Fig. 2A). These results are consistent with previous GCM studies of the mid-Holocene (e.g. Kutzbach & Street-Perrott 1985; Prell & Kutzbach 1992) and a wealth of proxy data (see Wright *et al.* 1993). The Asian interior is slightly drier than today and simulated soil moisture is lower. These results, obtained from the coupled atmosphere–ocean model, are consistent with atmosphere-only experiments performed using today's SST. The slight increase in aridity over the Asian interior during the Holocene is therefore related to orbital forcing and not to SST forcing.

In the LGM simulation, much of continental Asia is drier than present, particularly downstream of the Fennoscandian Ice Sheet (Fig. 2B). Increased precipitation along the front range of the Himalaya is a result of slight changes in the direction of the monsoon winds. In the tropics of the LGM simulation there is strong precipitation over Indonesia and a drying of the western Pacific. This pattern is consistent with a shift in convection from the western Pacific to the exposed Sunda shelf (which connects the islands of today's Indonesian archipelago and which was above sea level at the LGM). The impact of exposure/flooding of the massive Sunda shelf is that the entire tropical circula-

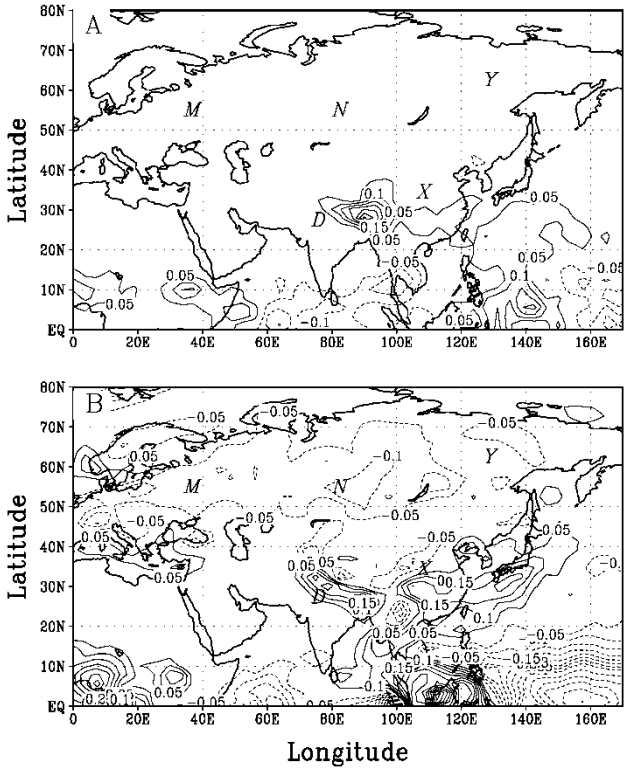

Fig. 2. Difference (experiment minus control) in annual mean precipitation (in cm/day) over Asia (A) during the mid-Holocene and (B) at the LGM. The contour interval in both panels is 0.05 cm/day.

tion over the Pacific basin is affected, as is the inter-annual variability associated with the El Niño Southern Oscillation (Bush & Fairbanks 2003). In particular, when the shelf is exposed there is increased subsidence and drying of the central Pacific through changes in the mean Walker circulation and there is a lengthening of the period of El Niño episodes.

If desert margins in the vicinity of the Chinese Loess Plateau are taken to have a particular value of soil moisture in the model then there is a statistically significant advance of the desert margin toward the southeast in the LGM simulation and a retreat toward the northwest in the mid-Holocene simulation (Bush *et al.* 2002). These numerical results agree qualitatively with the movement of desert margins inferred from sand content in loess deposits from the Plateau (Ding *et al.* 1999). From atmosphere-only integrations with modern SST, the desert margin would likely have been even further to the northwest at 9000 BP, since soil moisture in the region of the Loess Plateau is greater than at 6000 BP (Fig. 3).

Simulated annual mean snow cover over Asia is, in general, greater in the mid-Holocene than today, particularly in the northwest Himalaya and north-central Asia (Fig. 4A). At the LGM, there are large increases in snow accumulation in the eastern Himalaya and over the Fennoscandian Ice Sheet, but there is a reduction of snow accumulation over north-central to northeast Asia because of a rain shadow effect down-stream from the ice sheet (Fig. 4B). The westerly mid-latitude jet loses most of its moisture on the windward side of the ice and so is relatively dry once it reaches the Asian continental interior. In addition, the atmosphere is 10% drier in the LGM simulation, so large continental landmasses tend to be more arid inland from coastal regions.

Analysis of the changes in spatial pattern of snow accumulation (more snow in the eastern Himalaya at the LGM and more snow in the northwestern Himalaya during the mid-Holocene) has shown that they are caused by wind changes in the summer and winter south Asian monsoon (Bush 2002). In addition, it has been demonstrated that changes in the areal extent of snow accumulation can feed back on the strength of the monsoon itself (e.g. Dey *et al.* 1985; Bush 2000). Simulated changes in snow accumulation (which can be taken as a proxy for glacier expansion/contraction) are in accord with field data from these regions for these times (Benn & Owen 1998; Richards *et al.* 2000; Phillips *et al.* 2000; Taylor & Mitchell 2000). The numerical calculations therefore provide us with some

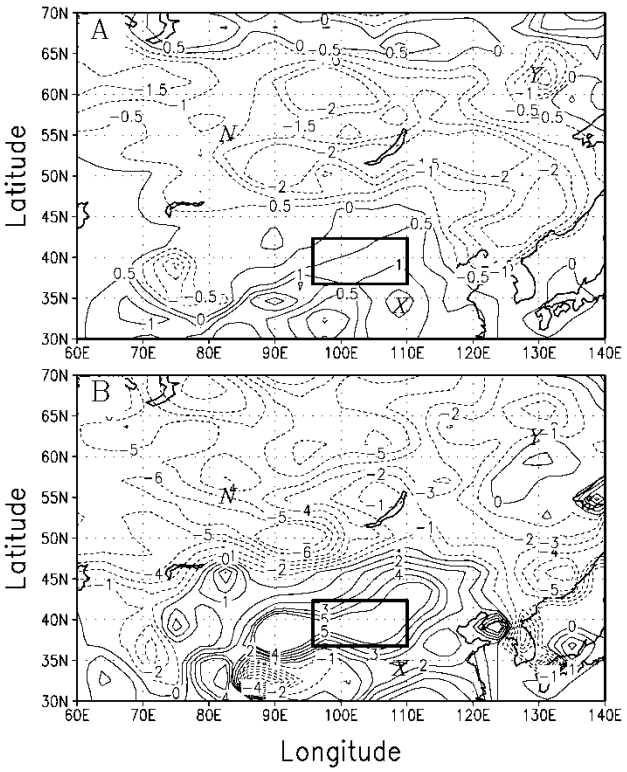

Fig. 3. Simulated difference (experiment minus control) in soil moisture at (A) 6000 BP and (B) 9000 BP. Units are centimeters of water. The rectangular box shown in both panels denotes the region of the modern desert margin, where the margin is taken to have soil moisture values of 2 cm.

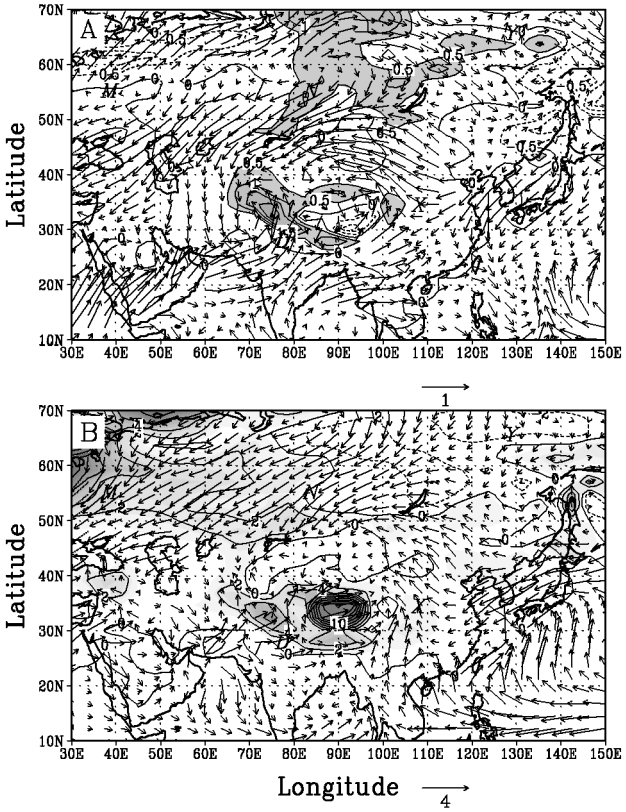

Fig. 4. Differences (experiment minus control) in annual mean snow accumulation (contours) and surface winds (arrows) (A) during the mid-Holocene and (B) at the LGM. Snow accumulation is given in terms of equivalent water amount (cm) with a contour interval of 0.5 cm in (A) and 2 cm in (B). Shading has been used to highlight positive snow accumulation differences, with darker shading indicating higher values. Wind vectors are scaled in m/s and are scaled as shown below each panel.

insight into the spatial and temporal variability of glacier growth in the Himalaya: changes in monsoon wind speed and direction can alter the amount of snow accumulation at a given location. This fact helps to explain why glacier expansion in some regions of the Himalaya does not necessarily correlate with northern hemisphere ice sheet volume. Despite significant increases in accumulation in the eastern Himalaya and along the entire front range, accumulation is relatively small across the western Tibetan Plateau. Simulated changes are not uniform across the entire Tibetan Plateau, and this fact may help explain the degree of spatial variability observed in lake levels across the Plateau (see Lehmkuhl & Haselein 2000). Colder temperatures across central Asia are conducive to the expansion of glaciers in the Altai (e.g. Lehmkuhl & Lang 2001) and Ural (e.g. Astakhov 1997) mountains, although only in the latter region is there a significant increase in simulated snow accumulation.

Simulated precipitation changes are caused by differences in the zones of convergence and divergence generated by changes in the atmospheric general circulation. It is therefore instructive to examine how and why the atmospheric winds were different over Asia. The difference in annual mean winds on the 850 mb surface indicate a stronger monsoon flow in the mid-Holocene simulation as well as stronger trade easterlies over the western Pacific (Fig. 5A). The stronger monsoon winds are a result of increased pressure gradients created in the more seasonal climate, and increased Pacific easterlies are associated with a more La Niña-like climatology. These wind changes correlate well with the differences in precipitation (cf. Fig. 2). In the LGM simulation, the jet stream is partially blocked by the Fennoscandian Ice Sheet and so westerlies over the continental interior are weaker than present (Fig. 5B). There is strong wind convergence and precipitation over the Sunda shelf because the exposed shelf is a tropical heat source that triggers convection and precipitation.

Discussion

Atmospheric GCMs with specified SST have been

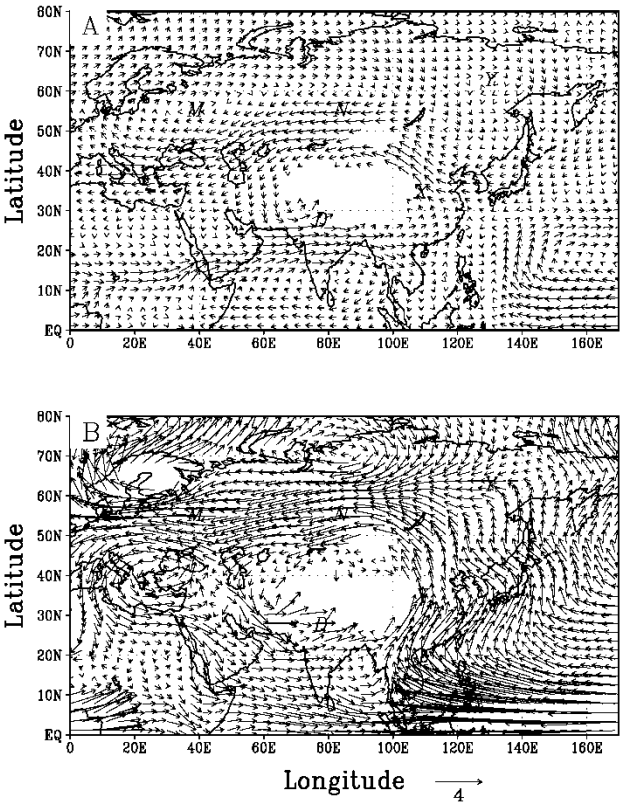

Fig. 5. Difference (experiment minus control) in the 850 mb winds over Asia (A) during the mid-Holocene and (B) at the LGM. Winds are not plotted where topographic height exceeds the 850 mb surface (e.g. over the Himalaya). The units are m/s and the wind vectors in both panels are scaled as shown below the bottom panel.

enormously useful in gaining insight into changes in atmospheric winds and temperatures during glacial and interglacial periods. Coupled atmosphere–ocean GCMs take the next step and determine how such changes in atmospheric circulation affect the ocean and how the coupled atmosphere–ocean dynamics are affected. Further development of coupled GCMs continues but they are at present sufficiently reliable for their results to be noted by government policy decision-makers (Grassl 2000).

We have investigated the climates in which northern hemisphere ice sheets evolved using an atmosphere-only GCM and a fully coupled atmosphere–ocean GCM. The focus has been the climate over the Asian continent, but it must be kept in mind that the climate system is global and that regional climate can be affected by geographically remote regions through atmospheric and oceanic teleconnections. One region that plays a fundamental role in maintaining global climate is the tropical Pacific Ocean. It covers approximately one-sixth of the surface area of our planet and semi-periodically undergoes the El Niño Southern Oscillation (ENSO) that changes regional SST by up to 10–12°C and alters the global atmospheric general circulation. SST in the tropical Pacific therefore provides a fundamental boundary condition for the atmosphere. Unfortunately, the present paucity of proxy climate data from the tropical Pacific has left open to debate the question of how tropical SST evolved during the late Quaternary.

Modelling studies are therefore a means of quantifying the range of possible values of tropical SST. For example, using the atmospheric GCM it has been shown that Pacific SST forcing can dominate orbital forcing of the south Asian monsoon (Bush 2001a) and, since there is a wealth of proxy data for monsoon strength, this fact places constraints on how warm or cold the SST may have been during the early Holocene. Nevertheless, new data (e.g. Andrus *et al.* 2002) and efforts to understand the dynamics linking the amount of mid-latitude eddy activity, the strength of the general circulation, and tropical Pacific SST (Bush 2001b) are expected to narrow the range of possibilities even further.

Tropical SST is linked to Asian climate primarily through the monsoon system. In modern climate, there is a strong correlation of weak monsoons with El Niño events and strong monsoons with La Niña events (e.g. Julian & Chervin 1978; Ropelewski & Halpert 1987, 1989). The dynamics underlying this connection, while still unclear, would probably have operated through the Late Quaternary, so changes in the climatological state of the tropical Pacific are extremely important for south Asian climate and hydrology. In simulations with the coupled atmosphere–ocean model, which produces slightly more La Niña-like conditions in the mid-Holocene (consistent with Galapagos and Andean records; Riedinger *et al.* 2002, Fontugne *et al.* 1999) and strong La Niña conditions at the LGM, a component of the changes in monsoon strength (and the concomitant changes in precipitation and snow accumulation) can therefore be attributed to tropical SST forcing. This point may be extrapolated further to state that within proxy records of monsoon intensity there is a component that is determined by tropical Pacific SST.

Overall, the major (simulated) differences in Asia's hydrological cycle at the LGM and during the mid-Holocene occurred in the region surrounding the Tibetan Plateau. While the continental interior had some changes (i.e. drying), the magnitude is small in comparison to the changes occurring in the vicinity of the Himalaya. Glaciation in the Himalaya is potentially of global importance because of the magnitude of solar radiation that is reflected back to space by tropical glaciers (Kuhle 1988). These simulations have therefore provided useful constraints on expected changes in Himalayan snow accumulation and precipitation to studies on glacier extent, surface runoff and geomorphology in the Himalaya system.

In contrast to the subtropical dominance of changes in the hydrological cycle, it is the higher latitudes that exhibit large changes in temperature through the late Quaternary. At the LGM over Asia, this result is a direct consequence of the Fennoscandian Ice Sheet upwind of the continental interior. During the mid-Holocene, warmer high-latitude temperatures are directly related to orbital forcing. Changes of atmospheric temperature can have substantially long-lasting impacts on the dynamics and evolution of glaciers. Surface temperature changes can, for example, propagate into the interior of ice by diffusion or advection, thereby altering the ice viscosity and flow dynamics (e.g. Dahl-Jensen *et al.* 1998; Wohlleben 2003). High Arctic glaciers of Canada and Asia can therefore preserve within the ice the signatures of past temperature anomalies. The degree of preservation, however, depends on glacier dynamics. For example, a relatively small glacier such as White Glacier in the Canadian Arctic is ideal for preserving relatively small and recent temperature anomalies such as those associated with the Little Ice Age (Wohlleben 2003), whereas larger ice masses (e.g. Greenland) are ideal for recording large amplitude events such as the LGM. Simulated temperature anomalies over northern Asia at the LGM and during the mid-Holocene are large enough that their signatures should be evident in the temperature profiles of glaciers in, for example, northwestern Siberia.

Concluding remarks and directions for future research

Unfortunately, time slice calculations do not provide an evolutionary picture of how the climate evolved from one state to another. High resolution GCM simulations that cover the entire late Quaternary are ideal but are, at

present, beyond the scope of modern computers. For this reason, we focused on two time slices, the LGM and the mid-Holocene, and analyzed the ways in which the atmosphere–ocean dynamics differed from today. However, there are many other areas to which future research may be directed. In particular, the impact of glacial meltwater on ocean circulation and climate has been shown to have global significance, as best exemplified by the Younger Dryas event (e.g. Manabe & Stouffer 1995; Fanning & Weaver 1997; Rutter *et al.* 2000; Clark *et al.* 2001). In this scenario, North American glacial meltwater inhibits convection in the North Atlantic, cooling surface waters sufficiently to lower temperatures around the world. From the Asian continent, meltwater from the Fennoscandian Ice Sheet discharged into the North Sea could possibly have been large enough to create a similar effect (or to have amplified the effect from the Laurentide meltwater). In addition, meltwater pulses through the Aral, Caspian, Black and Mediterranean Sea system could also have been large enough to impact Mediterranean circulation and outflow to the Atlantic; the volume discharges during these events are only now being estimated (A. Tchepalyga, pers. comm. 2000). Future modelling studies will be necessary to determine if they were large enough to affect global climate.

Acknowledgements. – I thank the Natural Sciences and Engineering Research Council for support through both Discovery Grant 194151 and the Climate System History and Dynamics Project, as well as UNESCO for sponsoring International Geological Correlation Project 415. I also thank Edward Derbyshire and Norm Catto, who reviewed an earlier version of this manuscript and helped make the numerical results more accessible to a broader community. This is a contribution to IGCP 415 (Glaciation and Reorganization of Asia's Network of Drainage) co-edited by Professor Jim Teller.

References

Andrus, C. F. T., Crowe, D. E., Sandweiss, D. H., Reitz, E. J. & Romanek, C. S. 2002: Otolith delta O-18 record of mid-Holocene sea surface temperatures in Peru. *Science 295*, 1508–1511.

Astakhov, V. 1997: Late glacial events in the central Russian Arctic. *Quaternary International 41–2*, 17–25.

Benn, D. I. & Owen, L. A. 1998: The role of the Indian summer monsoon and the mid-latitude westerlies in Himalayan glaciation: review and speculative discussion. *Journal of the Geological Society 155*, 353–363.

Berger, A. 1992: Orbital variations and insolation database. *IGBP PAGES/World Data Center—A for Paleoclimatology Data Contribution Series no. 92–007* NOAA/NGDC Paleoclimatology Program, Boulder, CO.

Berger, A. & Loutre, M. F. 1991: Insolation values for the climate of the last 10 million years. *Quaternary Science Reviews 10*, 297–317.

Braconnot, P., Joussaume, S., de Noblet, N. & Ramstein, G. 2000: Mid-Holocene and Last Glacial Maximum African monsoon changes as simulated within the Paleoclimate Modelling Intercomparison Project. *Global and Planetary Change 26*, 51–66.

Broccoli, A. J. & Manabe, S. 1987: The influence of continental ice, atmospheric CO_2, and land albedo on the climate of the last glacial maximum. *Climate Dynamics 1*, 87–99.

Broccoli, A. J. & Marciniak, E. P. 1996: Comparing simulated glacial climate and paleodata: a reexamination. *Paleoceanography 11*, 3–14.

Bush, A. B. G. 1999: Assessing the impact of mid-Holocene insolation on the atmosphere–ocean system. *Geophysical Research Letters 26*, 99–102.

Bush, A. B. G. 2000: A positive feedback mechanism for Himalayan glaciation. *Quaternary International 65–6*, 3–13.

Bush, A. B. G. 2001a: Pacific sea surface temperature forcing dominates orbital forcing of the early Holocene monsoon. *Quaternary Research 55*, 25–32.

Bush, A. B. G. 2001b: Simulating climates of the Last Glacial Maximum and of the mid-Holocene: wind changes, atmosphere–ocean interactions, and the tropical thermocline. *AGU Monograph Series 126 (The Oceans and Rapid Climate Change: Past, Present, and Future)*, 135–144.

Bush, A. B. G. 2002: A comparison of simulated monsoon circulations and snow accumulation during the mid-Holocene and at the Last Glacial Maximum. *Global and Planetary Change 32*, 331–347.

Bush, A. B. G. & Fairbanks, R. G. 2003: Exposing the Sunda shelf: tropical responses to eustatic sea level change. *Journal of Geophysical Research – Atmospheres 108(D15)*, 4446, doi: 10.1029/2002JD003027.

Bush, A. B. G. & Philander, S. G. H. 1998: The role of ocean–atmosphere interactions in tropical cooling during the Last Glacial Maximum. *Science 279*, 1341–1344.

Bush, A. B. G. & Philander, S. G. H. 1999: The climate of the Last Glacial Maximum: results from a coupled atmosphere–ocean general circulation model. *Journal of Geophysical Research 104*, 24,509–24,525.

Bush, A. B. G., Rokosh, D., Rutter, N. W. & Moodie, T. B. 2002: Desert margins near the Chinese Loess Plateau during the mid-Holocene and at the Last Glacial Maximum: a model-data intercomparison. *Global and Planetary Change 32*, 361–374.

Clark, P. U., Marshall, S. J., Clarke, G. V. C., Hostetler, S. W., Licciardi, J. M. & Teller, J. T. 2001: Freshwater forcing of abrupt climate change during the last glaciation. *Science 293*, 283–287.

CLIMAP (Climate: Long-Range Investigation, Mapping, and Prediction) Project Members 1981: Seasonal reconstructions of the Earth's surface at the last glacial maximum. *Map and Chart Series MC–36*. Geological Society of America, Boulder, CO.

Colinvaux, P. A., De Oliveira, P. E., Moreno, J. E., Miller, M. C. & Bush, M. B. 1996: A long pollen record from lowland Amazonia: forest and cooling in glacial times. *Science 274*, 85–88.

Colman, S. M., Peck, J. A., Karabanov, E. B., Carter, S. J., Bradbury, J. P., King, J. W. & Williams, D. F. 1995: Continental climate response to orbital forcing from biogenic silica records in Lake Baikal. *Nature 378*, 769–771.

Dahl-Jensen, D., Mosegaard, K., Gundestrup, N., Clow, G. D., Johnsen, S. J., Hansen, A. W. & Balling, N. 1998: Past temperatures directly from the Greenland Ice Sheet. *Science 282*, 268–271.

Dey, B., Kathuria, S. N. & Bhanu Kumar, O. S. R. U. 1985: Himalayan summer snow cover and withdrawal of the Indian summer monsoon. *Journal of Climatology and Applied Meteorology 24*, 865–868.

Ding, Z. L., Sun, J. M., Rutter, N. W., Rokosh, D. & Liu, T. S. 1999: Changes in sand content of loess deposits along a north–south transect of the Chinese Loess Plateau and the implications for desert variations. *Quaternary Research 52*, 56–62.

Fairbanks, R. G. 1989: A 17,000-year glacio-eustatic sea level record: influence of glacial melting rates on Younger Dryas event and deep-ocean circulation. *Nature 342*, 637–642.

Fanning, A. F. & Weaver, A. J. 1996: An atmospheric energy–moisture balance model: climatology, interpentadal climate change, and coupling to an ocean general circulation model. *Journal of Geophysical Research 101*, 15, 111–15, 128.

Fanning, A. F. & Weaver, A. J. 1997: Temporal–geographical melt-

water influences on the North Atlantic Conveyor: implications for the Younger Dryas. *Paleoceanography 12*, 307–320.
Fontugne, M., Usselmann, P., Lavallée, M., Julien, M. & Hatté, C. 1999: El Niño variability in the coastal desert of southern Peru during the mid-Holocene. *Quaternary Research 52*, 171–179.
Gordon, C. T. & Stern, W. 1982: A description of the GFDL global spectral model. *Monthly Weather Review 110*, 625–644.
Grassl, H. 2000: Status and improvements of coupled general circulation models. *Science 288*, 1991–1997.
Guilderson, T. P., Fairbanks, R. G. & Rubenstone, J. L. 1994: Tropical temperature variations since 20,000 years ago: modulating interhemispheric climate change. *Science 263*, 663–665.
Hall, N. M. J., Valdes, P. J. & Dong, B. 1996: The maintenance of the last great ice sheets: a UGAMP GCM study. *Journal of Climate 9*, 1004–1019.
Hope, G. S., Peterson, J. A., Radok, U. & Allison, I. 1976: *The Equatorial Glaciers of New Guinea*. 205 pp. A. A. Balkema, Rotterdam.
Julian, P. R. & Chervin, R. M. 1978: A study of the Southern Oscillation and Walker circulation phenomenon. *Monthly Weather Review 106*, 1433–1451.
Kageyama, M., Peyron, O., Pinot, S., Tarasov, P., Guiot, J., Joussaume, S. & Ramstein, G. 2001: The Last Glacial Maximum climate over Europe and western Siberia: a PMIP comparison between models and data. *Climate Dynamics 17*, 23–43.
Keshavamurty, R. N. 1982: Response of the atmosphere to sea surface temperature anomalies over the equatorial Pacific and the teleconnections of the Southern Oscillation. *Journal of the Atmospheric Sciences 39*, 1241–1259.
Kitoh, A., Murakami, S. & Koide, H. 2001: A simulation of the last glacial maximum with a coupled atmosphere–ocean GCM. *Geophysical Research Letters 28*, 2221–2224.
Kuhle, M. 1988: The Pleistocene glaciation of Tibet and the onset of Ice Ages: an autocycle hypothesis. *GeoJournal 17.4*, 581–595.
Kutzbach, J. E. & Guetter, P. J. 1986: The influence of changing orbital parameters and surface boundary conditions on climate simulations for the past 18,000 years. *Journal of the Atmospheric Sciences 43*, 1726–1759.
Kutzbach, J. E. & Otto-Bliesner, B. L. 1982: The sensitivity of the African–Asian monsoonal climate to orbital parameter changes for 9000 years B.P. in a low-resolution general circulation model. *Journal of the Atmospheric Sciences 39*, 1177–1188.
Kutzbach, J. E. & Street-Perrott, F. A. 1985: Milankovitch forcing of fluctuations in the level of tropical lakes from 18–0 kyr BP. *Nature 317*, 130–134.
Kuzmin, M. I., Grachev, M. A., Williams, D., Kawai, T., Horie, Sh. & Oberhensli, H. 1997: A continuous record of paleoclimates for the last 4.5 Ma on Lake Baikal (first data). *Geologiya I Geofizika 38*, 1021–1023.
Lamoureux, S., England, J. H., Sharp, M. J. & Bush, A. B. G. 2001: A varve record of increased Little Ice Age rainfall associated with volcanic activity, Arctic Archipelago, Canada. *Holocene 11*, 243–249.
Lehmkuhl, F. & Haselein, F. 2000: Quaternary paleoenvironmental change on the Tibetan Plateau and adjacent areas (Western China and Western Mongolia). *Quaternary International 65/66*, 121–145.
Lehmkuhl, F. & Lang, A. 2001: Geomorphological investigations and luminescence dating in the southern part of the Khangay and the Valley of the Gobi Lakes (Central Mongolia). *Journal of Quaternary Science 16*, 69–87.
Levitus, S. 1982: Climatological atlas of the world ocean. *NOAA Prof. Paper 13* U.S. Government Printing Office, Washington, D.C173.
MacDonald, G. M., Velichko, A. A., Kremenetski, C. V., Borisova, O. K., Goleva, A. A., Andreev, A. A., Cwynar, L. C., Riding, R. T., Forman, S. L., Edwards, T. W. D., Aravena, R., Hammarlund, D., Szeicz, J. M. & Gattaulin, V. N. 2000: Holocene treeline history and climate change across northern Eurasia. *Quaternary Research 53*, 302–311.
Mahowald, N., Kohfeld, K., Hansson, M., Balkanski, Y., Harrison, S. P., Prentice, I. C., Schulz, M. & Rodhe, H. 1999: Dust sources and deposition during the last glacial maximum and current climate: a comparison of model results with paleodata from ice cores and marine sediments. *Journal of Geophysical Research – Atmospheres 104(D13)*, 15895–15916.
Manabe, S. & Broccoli, A. J. 1985: A comparison of climate model sensitivity with data from the last glacial maximum. *Journal of the Atmospheric Sciences 42*, 2643–2651.
Manabe, S. & Hahn, D. G. 1977: Simulation of the tropical climate of an ice age. *Journal of Geophysical Research 82*, 3889–3911.
Manabe, S. & Stouffer, R. J. 1995: Simulation of abrupt climate-change induced by fresh-water input to the North Atlantic Ocean. *Nature 378*, 165–167.
Otto-Bleisner, B. L. 1999: El Niño/La Niña and Sahel precipitation during the middle Holocene. *Geophysical Research Letters 26*, 87–90.
Pacanowski, R. C., Dixon, K. & Rosati, A. 1991: *The GFDL Modular Ocean Model user guide, GFDL Ocean Group Technical Report 2* Geophysical Fluid Dynamics Laboratory, Princeton, N.J.
Peltier, W. R. 1994: Ice age paleotopography. *Science 265*, 195–201.
Phillips, W. M., Sloan, V. F., Shroder, Jr., J. F., Sharma, P., Clarke, M. L. & Rendell, H. M. 2000: Asynchronous glaciation at Nanga Parbat, northwestern Himalaya Mountains, Pakistan. *Geology 28*, 431–434.
Pinot, S., Ramstein, G., Harrison, S. P., Prentice, I. C., Guiot, J., Stute, M. & Joussaume, S. 1999: Tropical paleoclimates at the Last Glacial Maximum: comparison of Paleoclimate Modeling Intercomparison Project (PMIP) simulations and paleodata. *Climate Dynamics 15*, 857–874.
Prell, W. L. & Kutzbach, J. E. 1992: Sensitivity of the Indian monsoon to forcing parameters and implications for its evolution. *Nature 360*, 647–652.
Prentice, I. C. & Webb, III, T. 1998: BIOME 6000: reconstructing global mid-Holocene vegetation patterns from palaeoecological records. *Journal of Biogeography 25*, 997–1005.
Prentice, I. C., Harrison, S. P., Jolly, D. & Guiot, J. 1998: The climate and biomes of Europe at 6000 yr BP: comparison of model simulations and pollen-based reconstructions. *Quaternary Science Reviews 17*, 659–668.
Richards, B. W., Owen, L. A. & Rhodes, E. J. 2000: Timing of Late Quaternary glaciations in the Himalaya of northern Pakistan. *Journal of Quaternary Science 15*, 283–297.
Riedinger, M. A., Steinitz-Kannan, M., Last, W. M. & Brenner, M. 2002: A similar to 6100 C-14 yr record of El Niño activity from the Galapagos Islands. *Journal of Paleolimnology 27*, 1–7.
Rind, D. & Peteet, D. 1985: Terrestrial conditions at the last glacial maximum and CLIMAP sea-surface temperature estimates: are they consistent? *Quaternary Research 24*, 1–22.
Ropelewski, C. F. & Halpert, M. S. 1987: Global and regional scale precipitation patterns associated with the El Niño Southern Oscillation. *Monthly Weather Review 115*, 1606–1626.
Ropelewski, C. F. & Halpert, M. S. 1989: Precipitation patterns associated with the high index phase of the Southern Oscillation. *Journal of Climate 2*, 268–284.
Rutter, N. W. 1992: Presidential Address, XIII INQUA Congress 1991: Chinese loess and global change. *Quaternary Science Reviews 11*, 275–281.
Rutter, N. W., Weaver, A. J., Rokosh, D., Fanning, A. F. & Wright, D. G. 2000: Data-model comparison of the Younger Dryas event. *Canadian Journal of Earth Sciences 37*, 811–830.
Schrag, D. P., Hampt, G. & Murray, D. W. 1996: Pore fluid constraints on the temperature and oxygen isotopic composition of the glacial ocean. *Science 272*, 1930–1932.
Stute, M., Forster, M., Frischkorn, H., Serejo, A., Clark, J. F., Schlosser, P., Broecker, W. S. & Bonani, G. 1995: Cooling of Tropical Brazil (5°C) during the last glacial maximum. *Science 269*, 379–383.
Taylor, P. J. & Mitchell, W. A. 2000: The Quaternary glacial history

of the Zanskar Range, north-west Indian Himalaya. *Quaternary International 65–5*, 81–99.

Thompson, L. G., Mosley-Thompson, E., Davis, M. E., Lin, P.-N., Henderson, K. A., Cole-Dai, J., Bolzan, J. F. & Liu, K.-B. 1995: Late glacial stage and Holocene tropical ice core records from Huascarán, Peru. *Science 269*, 46–50.

Weaver, A. J., Eby, M., Fanning, A. F. & Wiebe, E. C. 1998: Simulated influence of CO_2, orbital forcing and ice sheets on the climate of the last glacial maximum. *Nature 394*, 847–853.

Wetherald, R. W. & Manabe, S. 1988: Cloud feedback processes in a general circulation model. *Journal of the Atmospheric Sciences 45*, 1397–1415.

Wohlleben, T. M. H. 2003: *Atmosphere–Ice Interactions in the Canadian High Arctic*. Ph.D. dissertation, University of Alberta, 145 pp.

Wright, H. E, Jr., Kutzbach, J. E., Webb, III, T., Ruddiman, W. F., Street-Perrott, F. A. & Bartlein, P. J. (eds.) 1993: *Global Climates Since the Last Glacial Maximum*. 569 pp. University of Minnesota Press, Minneapolis.